J Mater Sci (2010) 45:1604–1609
DOI 10.1007/s10853-009-4134-z

Intercalation of methylene blue into layered potassium titanoniobate $KTiNbO_5$: characterization and electrochemical investigation

Xiaobo Zhang · Chao Liu · Lin Liu · Dongen Zhang · Tianlin Zhang · Xingyou Xu · Zhiwei Tong

Received: 16 July 2009 / Accepted: 16 December 2009 / Published online: 30 December 2009

Abstract Methylene blue (MB) was intercalated into layered potassium titanoniobate ($KTiNbO_5$) through a guest–guest exchange method by use of the intercalation compound n-$C_4H_9NH_3^+$–$TiNbO_5$ as a precursor. The MB^+/H^+–$TiNbO_5$ nanocomposite has been characterized by XRD, SEM, IR, TGA, UV, elemental analysis, and electrochemical cyclic voltammetric measurements. From the XRD and elemental analysis results, we proposed that the MB^+ cations formed a single layer standing vertically to the titanoniobate nanosheets together with H^+. The CV curves of the MB^+/H^+–$TiNbO_5$ nanocomposite thin film exhibited a fine diffusion-controlled redox process, which hints the possibility of being utilized as an electrode modifying material.

Introduction

Recently, there has been a tremendous increase in interest in nanosized two-dimensional semiconducting metal oxides due to their unique laminar structure. Intercalation of metal ions [1], transition metal oxides [2], and organic ions [3] into the interlayer of layered metal oxides may produce new hybrid materials, which can be used as photocatalysts and nanoscale devices. Potassium titanoniobate ($KTiNbO_5$) is a unique layered semiconducting material having high photocatalytic efficiency for decomposition of water into H_2 and O_2 [4]. Figure 1 shows the layer structure of $KTiNbO_5$, edge-sharing octahedra of NbO_6 and TiO_6 form zigzag strings, and corner-sharing octahedra along the b-axis construct sheets are perpendicular to the c-axis, exchangeable K^+ ions exist in the interlayer [5]. Ion-exchange properties of layered $KTiNbO_5$ was first reported in 1979 [6], and from then on, the intercalation of $KTiNbO_5$ with metal oxides [7], aliphatic amines [8], methylviologen [9], porphyrin [10], polyaniline [11], and polyfluorinated cationic azobenzene [12] have been prepared successfully, the photocatalytic, photoelectrochemical, and photo-induced electron-transfer behaviors of the intercalation nanocomposites have been extensively investigated. However, the electrochemical behaviors of the intercalated ions, especially the dye cations were not popularly reported, the prospective utilization of the nanocomposites as modified electrodes was not widely discussed.

Methylene blue (MB) (Fig. 2) is a cationic, thiazine dye with plane structure, which is widely used for electrochemical applications, such as catalyst-mediator in electrochemical biosensors or redox indicator in electrochemical determinations. However, MB is a low molecular weight water-soluble mediator, which may affect the stability of biosensors. For this reason, immobilization of MB with various matrices such as silicate [13], barium phosphate [14], TiO_2 [15], mordenite-type zeolite [16], zirconium phosphate [17], layered manganese oxide [18] was studied to

X. Zhang
Key Laboratory of Soft Chemistry and Functional Materials, Ministry of Education, Nanjing University of Science and Technology, Nanjing 210094, People's Republic of China

X. Zhang · C. Liu · L. Liu · D. Zhang · T. Zhang · X. Xu · Z. Tong
Department of Chemical Engineering, Huaihai Institute of Technology, Lianyungang 222005, People's Republic of China

Z. Tong (✉)
SORST, Japan Science and Technology Agency (JST), Kawaguchi Center Building 4-1-8, Kawaguchi-shi, Saitama 332-0012, Japan
e-mail: zhiweitong575@hotmail.com

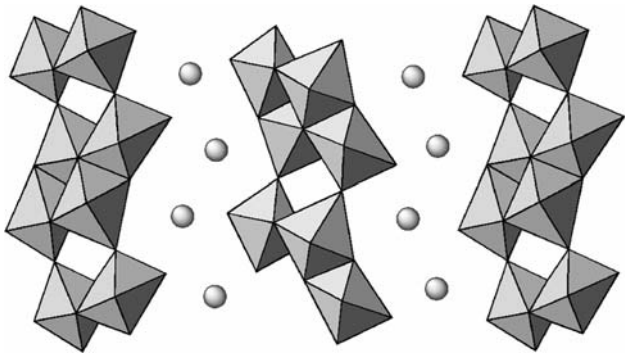

Fig. 1 Structure of $KTiNbO_5$. *Squares* represent the TiO_6 (and NbO_6) octahedra, and *circles* indicate the exchangeable cation K^+ in the interlayer

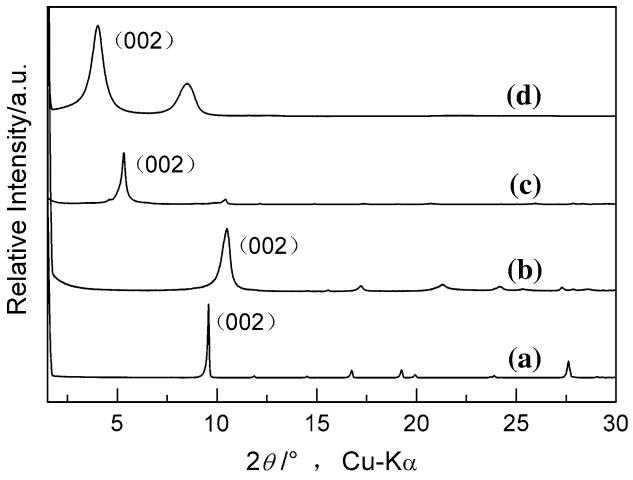

Fig. 3 The X-ray diffraction patterns of (*a*) $KTiNbO_5$, (*b*) $HTiNbO_5$, (*c*) n-$C_4H_9NH_3^+$–$TiNbO_5$, and (*d*) MB^+/H^+–$TiNbO_5$

overcome this shortcoming. MB^+ intercalated layered niobate ($K_4Nb_6O_{17}$) has also been studied [19, 20] and we have reported the electrochemical behavior of intercalated MB^+ cation [20], but the intercalation of MB into the $KTiNbO_5$ has not been studied yet.

In this paper, we report a guest–guest ion exchange method for preparing MB^+/H^+–$TiNbO_5$ nanocomposite by use of the intercalation compound n-$C_4H_9NH_3^+$–$TiNbO_5$ as a precursor. The MB^+/H^+–$TiNbO_5$ nanocomposite was characterized by X-ray diffraction, SEM, IR, TGA, elemental analysis, and UV spectroscopy. The electrochemical behaviors of MB^+/H^+–$TiNbO_5$ nanocomposite were studied, the stability of the nanomaterial was proved.

Experimental

Materials

Analytical TiO_2 (anatase), Nb_2O_5, and K_2CO_3 were purchased from Sinopharm Chemical Reagent Co., Ltd, *n*-butylamine and methylene blue were purchased from Tokyo Kasei, all reagents were used without further purification.

The layered potassium titanoniobate ($KTiNbO_5$) was prepared by calcination of a 1:2:1 M ratio mixture of K_2CO_3, TiO_2, and Nb_2O_5 at 1150 °C for 24 h, according to the previous literature [5]. The direct intercalation of $KTiNbO_5$ with MB^+ ion is difficult, so a guest exchange reaction with the n-$C_4H_9NH_3^+$–$TiNbO_5$ intermediate was performed to obtain the MB^+/H^+–$TiNbO_5$ nanocomposite. The n-$C_4H_9NH_3^+$–$TiNbO_5$ hybrid was prepared as follows: 1 g of the powder potassium titanoniobate was treated three times with 1 mol dm^{-3} HCl (100 mL each) for 24 h at room temperature; the resulting titanoniobic acid powder was washed with deionized water until free of Cl^{-1} and then air-dried; 0.5 g of the white titanoniobic acid powder was sealed in a 200-mL glass ampoule with 15 mL of an aqueous 50% *n*-butylamine solution and stirred for 2 weeks at room temperature, then the precipitate powder was washed with alcohol (5 times) to obtain n-$C_4H_9NH_3^+$–$TiNbO_5$ hybrid. 0.5 g of the white n-$C_4H_9NH_3^+$–$TiNbO_5$ powder was allowed to react with 30 mL of aqueous 5 mmol dm^{-3} MB^+ solution in a 50-mL glass ampoule for 2 weeks. The resultant solution was centrifuged and washed with deionized water several times to obtain a blue powder MB^+/H^+–$TiNbO_5$ nanocomposite.

Characterizations

Characterizations of the MB^+/H^+–$TiNbO_5$ hybrid were carried out by means of X-ray diffraction, SEM, IR, TGA, UV, and elemental analysis, as well as electrochemical analysis. XRD patterns were collected with a M21X (MAC

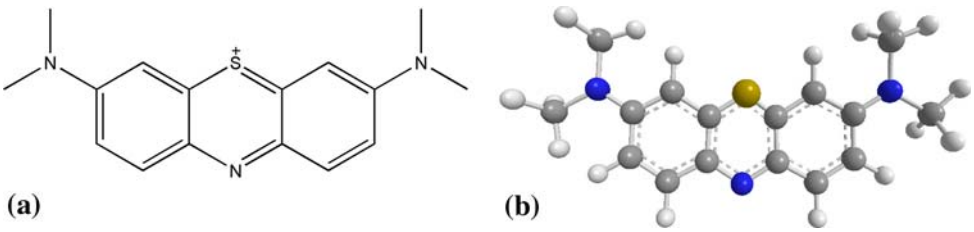

Fig. 2 The molecular structure (**a**) and structural model (**b**) of methylene blue cation

Co., Ltd) diffractometer with monochromatic CuK_α radiation ($\lambda = 0.15406$ nm) with 2θ going from 1.5° to 30° in 1° steps. Scanning electron microscopic (SEM) image was taken with a JSM-6390 apparatus (JEOL) for the Au-coated sample. IR spectra were measured using KBr pellets on a WGH-30/6 double-beam IR-spectrometer. Thermal gravimetric analysis (TGA) was carried out on a Shimadzu DTG-60 apparatus at an average heating rate of 20 °C min^{-1} from room temperature to 800 °C in air. UV absorption spectra were carried out using a UV–vis spectrometer (UV-2550). The composition of the MB^+/H^+–$TiNbO_5$ hybrid was performed using a Perkin Elmer 2400-CHN elemental analyzer. The electrochemical experiments were carried out in a conventional three-electrode electrochemical cell at room temperature, with a platinum wire electrode as the counter electrode and a saturated calomel electrode (SCE) as the reference electrode. For preparing the nanocomposite modifying working electrode, 0.1 g of the MB^+/H^+–$TiNbO_5$ nanocomposite was dispersed in 1 mL ultra pure water to obtain a blue solution, then 5 μL of the MB^+/H^+–$TiNbO_5$ solution was cast on the surface of a glass carbon electrode (GCE) and dry in air. The acting electrolyte was 0.1 mol L^{-1} HCl solution. CV scans were carried out on a CHI600b electrochemical workstation at scan rate of 50–500 mV s^{-1} under highly pure nitrogen atmosphere.

Results and discussion

Characterization of MB^+/H^+–$TiNbO_5$ nanocomposite

The XRD patterns in Fig. 3a and b exhibit the interlayer spacing change from 0.92 to 0.85 nm after the protonation of $KTiNbO_5$. The sharp peaks indicate the high crystallinity of the product. The *n*-$C_4H_9NH_3^+$–$TiNbO_5$ hybrid has a d_{002} value of 1.65 nm (Fig. 3c), indicating the preintercalation of interlayer spacing by butylammonium ion. The substituent of MB^+ cation for *n*-$C_4H_9NH_3^+$ resulted in a larger interlayer spacing of MB^+/H^+–$TiNbO_5$ (2.20 nm), as can be seen in the XRD diffraction patterns in Fig. 3c,d. The basal spacing and the Δd values of these compounds are shown in Table 1. The net interlayer height of MB^+/H^+–$TiNbO_5$ was calculated as 1.70 nm by subtracting the thickness of the $TiNbO_5^-$ layer (0.5 nm for a single sheet) [21] from the observed basal spacing (2.20 nm). Figure 4 shows the micromorphology of the hybrid MB^+/H^+–$TiNbO_5$, the laminar structure of the titanoniobate still remains after the intercalation of the MB^+ cation; however, the exfoliation of the layers also happen, so crinkles can be seen at the edges of the layers.

The IR spectrum of the intercalate MB^+/H^+–$TiNbO_5$ is shown in Fig. 5c, with the spectra of MB and $KTiNbO_5$ for comparison. The stretching modes of the aromatic ring

Table 1 X-Ray powder diffraction data

Compound	d_{002} (nm)	Δd (nm)[a]
$KTiNbO_5$	0.92	–
$HTiNbO_5$	0.85	–
n-$C_4H_9NH_3^+$–$TiNbO_5$	1.65	1.15
MB^+/H^+–$TiNbO_5$	2.20	1.70

[a] Δd is the gallery height

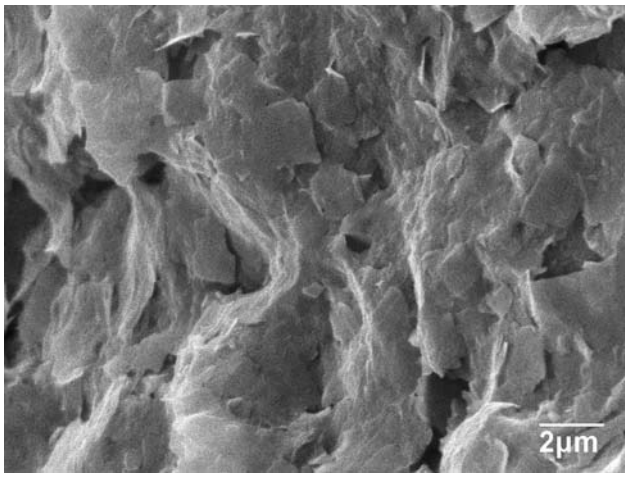

Fig. 4 SEM micrograph of MB^+/H^+–$TiNbO_5$ hybrid

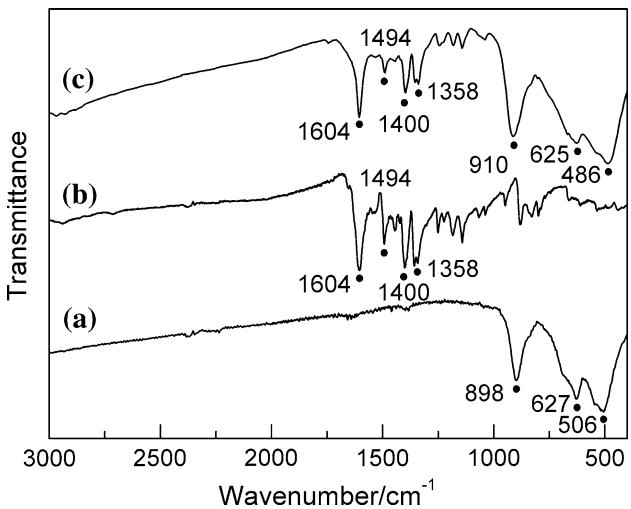

Fig. 5 IR spectra of (*a*) $KTiNbO_5$, (*b*) MB and (*c*) MB^+/H^+–$TiNbO_5$ nanocomposite

at 1604 cm^{-1} and 1494 cm^{-1}, the C–N symmetric stretch at 1400 cm^{-1}, the $-CH_3$ symmetric deformation at 1358 cm^{-1} are characteristic infrared absorption peaks of MB (Fig. 5b) [13, 15, 22], and the absorbance peaks between 500 and 1000 cm^{-1} belong to the Nb–O and Ti–O stretching vibration (Fig. 5a) [23]. The above results

confirm that MB has been intercalated into the interlayer spaces of titanoniobate successfully.

Based on the elemental analysis result (C, H, and N distribution of 14.25, 2.42, and 3.15%, respectively) for the MB^+/H^+–$TiNbO_5$ hybrid, the composition formula for the MB^+/H^+–$TiNbO_5$ hybrid can be calculated as $(MB^+)_{0.23}H_{0.77}TiNbO_5 \cdot 1.25H_2O$, in which the calculated C/N molar ratio, 5.28 (14.25/12:3.15/14 = 5.28), is in good agreement with the observed value, 5.33. The rectangular dimensions of MB molecular are approximately 1.70 nm × 0.76 nm × 0.325 nm [24] and the reported area of host layer surface per charge for the titanoniobate is 0.123 nm^2 [25]. The maximum amount of MB^+ cations standing as a monolayer perpendicularly to the interlayer is calculated as 0.123/(0.76 × 0.325) = 0.5 mol, while if the MB^+ cations lie with the long axis parallel to the $TiNbO_5^-$ layers, the maximum amount could be calculated as 0.123/(1.7 × 0.325) = 0.22 mol. Although the later model has an value of MB^+ cation similar to the observed value, 0.23, it is implausible because the Δd value of $TiNbO_5^-$ layers calculated from XRD data is 1.7 nm, which is too large for the monolayer arrangement of MB^+ with the long axis parallel to the $TiNbO_5^-$ layers, for the same reason, a bilayer model is also unrealistic. Considering the interlayer spacing of the intercalate and the H^+ exist in the interlayers, we suggest that the MB^+ cations might form a monolayer standing vertically to the titanoniobate nanosheets together with H^+.

Figure 6 gives the TGA curve of the MB^+/H^+–$TiNbO_5$ nanocomposite. We have reported the TG curve of $KTiNbO_5$ and there is little weight loss between 300 and 400 °C [26], so the weight loss of the host material is omitted and we explain the thermal behavior of the MB^+/H^+–$TiNbO_5$ nanocomposite with a two-step weight loss process. The first weight loss step from room temperature to 160 °C (7%) is believed to be the vaporization of the

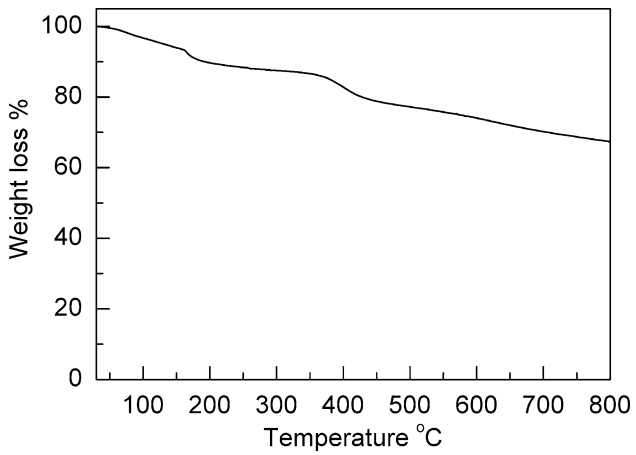

Fig. 6 TGA curve of MB^+/H^+–$TiNbO_5$ nanocomposite

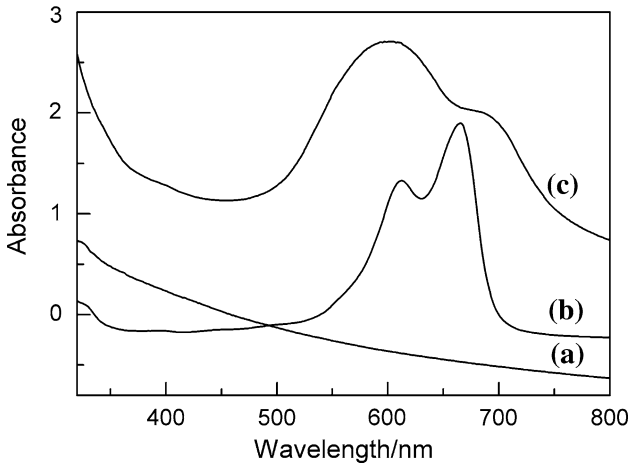

Fig. 7 UV spectra of n-$C_4H_9NH_3^+$–$TiNbO_5$ precursor (*a*), 0.5 m mol L^{-1} MB solution (*b*) and MB^+/H^+–$TiNbO_5$ nanocomposite (*c*)

intercalated water, the second weight loss from 160 to 650 °C (21%) is due to the decomposition of MB^+ cation in the nanocomposite interlayer. The total weight loss (28%) is consistent with the sum of the water and MB^+ cation content determined by the elemental analysis.

UV spectra of the precursor n-$C_4H_9NH_3^+$–$TiNbO_5$, 0.5 m mol L^{-1} MB solution and the MB^+/H^+–$TiNbO_5$ nanocomposites are shown in Fig. 7. UV–vis optical absorption of a typical MB^+/H^+–$TiNbO_5$ film presents a nonsymmetrical peak with a maximum absorbance at 600 nm and a shoulder at 695 nm (Fig 7c). Comparing with the UV spectrum of n-$C_4H_9NH_3^+$–$TiNbO_5$, it can be concluded that MB^+ cation is intercalated into spaces of $TiNbO_5^-$ layers. It is reported that there are several aggregates of MB in MB^+ aqueous solution, the typical absorbance peaks are at 650–675 nm for the monomer, at 605 nm for the dimer, and at 570–590 nm for trimers, tetramers, and still higher aggregates [13, 27–31]. Here, we ascribe the absorbance peak at 600 nm to the dye dimer and the peak at 695 nm to the presence of MB monomer. The position of the maximum and the shape of the signal suggest that MB is mainly present as dimers, while the proportion of monomers is comparably lower [24, 32].

Electrochemical behavior of MB^+/H^+–$TiNbO_5$ nanocomposite thin film

The CV curve of MB in aqueous solution at 100 mV s^{-1} scan rate is shown in Fig. 8a. There are a couple of sensitive oxidation/reduction peaks with redox potentials at 0.2 and 0.167 V, with the midpoint potential [$E_m = (E_{pa} + E_{pc})/2$] of 0.184 V. The peak separation [$\Delta E_p = (E_{pa} - E_{pc})$] is 33 mV, which is between the ΔE_p value of individual electron transfer reaction (59 mV) and

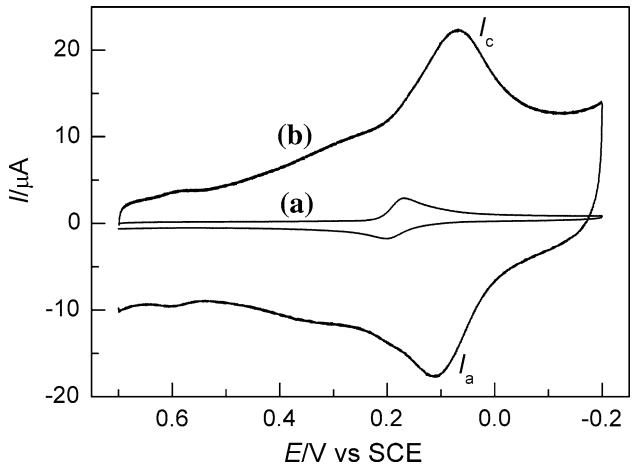

Fig. 8 Cyclic voltammograms of (*a*) MB (0.5 mmol L^{-1}) and (*b*) MB^+/H^+–$TiNbO_5$ thin film in 0.1 mol L^{-1}HCl solution, scan rate: 100 mV s^{-1}

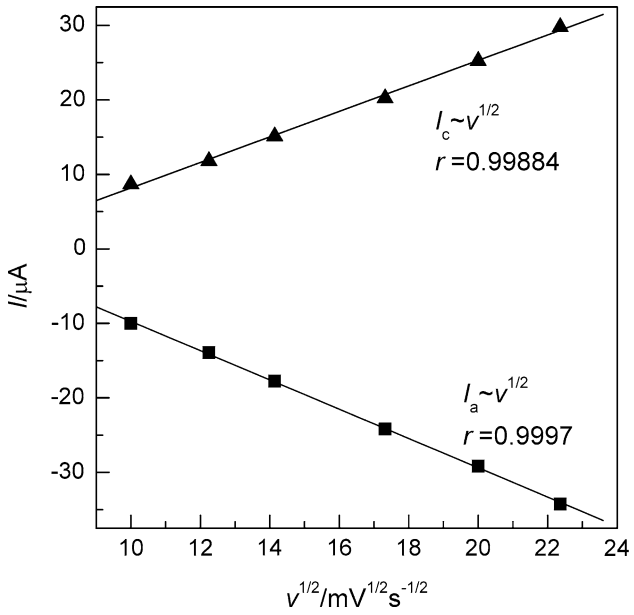

Fig. 10 $I \sim \upsilon^{1/2}$ relationships for MB^+/H^+–$TiNbO_5$ layer nanocomposite thin film in 0.1 mol L^{-1} HCl solution

two-electron transfer reaction (28.5 mV), indicating a two-step individual electron transfer reaction of MB dimer [33, 34]. For the typical MB^+/H^+–$TiNbO_5$ hybrid film on GCE, the redox potentials are at 0.114 and 0.071 V with a mid-point potential of 0.093 V and larger peak separation of 43 mV (Fig. 8b). The negative shift of E_m and increase of ΔE_p for the case of hybrid film is explained to be the result of the blocking effect of the hybrid film on the charge transfer of MB reaction [35]. The peak currents of the hybrid are much higher than that of MB in aqueous solution, which is due to the high concentration of the MB cations in the interlayer of the nanocomposite.

The cyclic voltammetric behaviors of MB^+/H^+–$TiNbO_5$ at different scan rates are shown in Fig. 9. There is a shift of E_{pc} to more negative values and a shift of E_{pa} to more positive values with increasing the scan rate. The redox peaks are assigned to a two-electron quasi-reversible redox process of MB dimer [17, 36–38]. The cathodic and anodic peak currents (I_c and I_a) are proportional to the square root of the scan rate (Fig. 10), which indicates a planar diffusion-controlled redox behavior of MB^+ cations in titanioniobate interlayer. The ΔE_p increased from 43 to 93 mV when the scan rate varied from 100 to 500 mV s^{-1}, indicating a slow electron diffusion process of the MB^+ cations in the interlayer space at high scan rates. This is due to the semiconducting nature of the titanoniobate matrix [17].

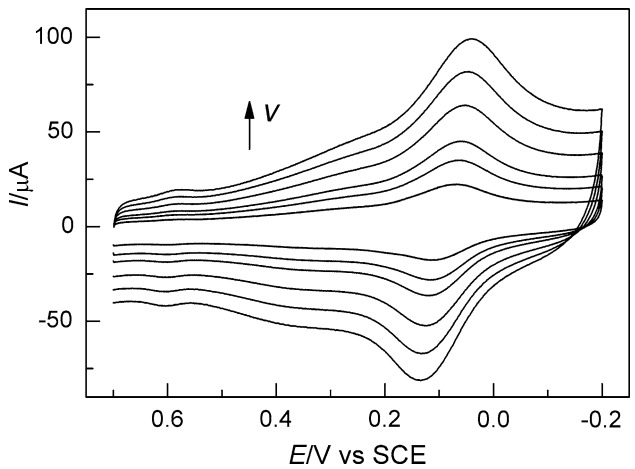

Fig. 9 CV curves of MB^+/H^+–$TiNbO_5$ thin film at different scan rates (100, 150, 200, 300, 400, 500 mV s^{-1} from inner to outer)

The ideal linear relationship in Fig. 10 indicates a fine mass transfer process, which hints the potential utilization of the MB^+/H^+–$TiNbO_5$ laminar nanocomposite as electrode modifying material. In order to test the electrochemical stability of the MB^+/H^+–$TiNbO_5$ hybrid film, the MB^+/H^+–$TiNbO_5$ nanocomposite modified-GCE was tested for five repeated circles at the scan rate of 50 mV s^{-1} again immediately after the former electrochemical cyclic voltammetric experiments. It can be seen from Fig. 11 that the MB^+/H^+–$TiNbO_5$ hybrid material are very stable in acid conditions, with almost no observable changes in both the peak current and the peak separation after five scan circles, which confirms the good immobilization of MB in titanoniobate interlayer spacing. It can be concluded that the excellent electrochemical stability and reproducibility of the nanocomposite are not affected by the presence of layered host material, and the MB^+/H^+–$TiNbO_5$ hybrid material possesses good opportunities for practical applications in electrochemistry.

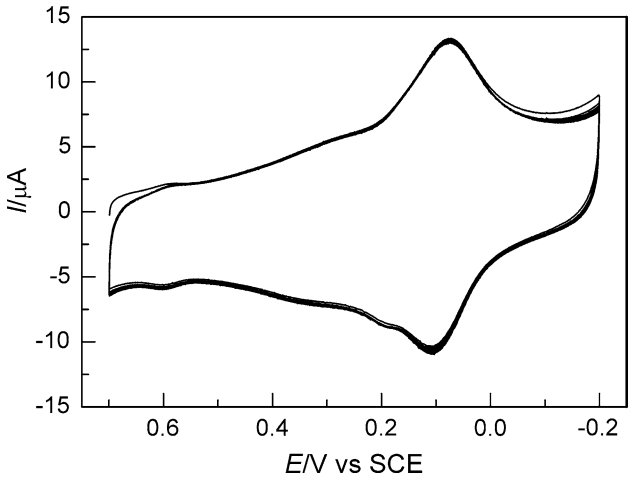

Fig. 11 Cyclic voltammograms upon five repeated scans of MB^+/H^+–$TiNbO_5$ hybrid in 0.1 mol L^{-1} HCl solution at scan rate of 50 mV s^{-1}

Conclusions

Layered nanocomposite MB^+/H^+–$TiNbO_5$ was synthesized through guest–guest ion exchange reaction with a precursor n-$C_4H_9NH_3^+$–$TiNbO_5$. The hybrid nanocomposite was characterized using XRD, SEM, IR, UV, TGA, elemental analysis, and electrochemical cyclic voltammetric investigation. Based on the XRD and elemental analysis results, we proposed that the MB^+ cations formed a single layer with its long axis standing vertically to the titanoniobate layers together with H^+. The cyclic voltammogram of the MB^+/H^+–$TiNbO_5$ nanocomposite film possessed a pair of distinct reductive and oxidative peaks, representing a two-electron redox process. The peak currents exhibited fine diffusion-controlled processes, and the electrochemical stability of the hybrid film was also proved. We predict that the novel MB^+/H^+–$TiNbO_5$ nanocomposite has potential capacity as electrode modifying material.

Acknowledgements This work was supported by a Grant-in-aid for Scientific Research from the Japan Society for the Promotion of Science (JSPS) and the CREST program of the Japan Science and Technology Agency (JST). We are grateful to young and middle aged academic leaders of Jiangsu Province universities' "blue and green blue project". This work is also supported by National Natural Science Foundation of China (Grant No. 50873042).

References

1. Nunes LM, de Souza AG, de Farias RF (2001) J Alloy Compd 319:94
2. Chatchai P, Murakami Y, Kishioka SY, Nosaka AY, Nosaka Y (2009) Electrochim Acta 54:1147
3. Takagi S, Eguchi M, Tryk DA, Inoue H (2006) J Photochem Photobiol C 7:104
4. Takahashi H, Kakihana M, Yamashita Y, Yoshida K, Ikeda S, Hara M, Domen K (1999) J Alloy Compd 285:77
5. Wadsley AD (1964) Acta Crystallogr 17:623
6. Rebbah H, Desgardin G, Raveau B (1979) Mater Res B 14:1125
7. Chen YS, Hou WH, Guo CX, Yan QJ, Chen Y (1997) J Chem Soc Dalton Trans 359
8. Rebbah H, Borel MM, Raveau B (1980) Mater Res Bull 15:317
9. Nakato T, Miyata H, Kuroda K, Kato C (1988) React Solid 6:231
10. Tong ZW, Shichi T, Takagi K (2002) J Phys Chem B 106:13306
11. Yang G, Hou WH, Feng XM, Xu L, Liu YG, Wang G, Ding WP (2007) Adv Funct Mater 17:401
12. Tong ZW, Sasamoto S, Shimada T, Takagi S, Tachibana H, Zhang XB, Tryk DA, Inoue H (2008) J Mater Chem 18:4641
13. Yao H, Li N, Xu S, Xu JZ, Zhu JJ, Chen HY (2005) Biosensors Bioelectronics 21:372
14. Lazarin AM, Airoldi C (2004) Anal Chim Acta 523:89
15. David GT, Xavier D, Nieves CP, José AA (2007) J Photochem A Photobiol Chem 187:45
16. Arvand M, Sohrabnezhad SH, Mousavi MF, Shamsipur M, Zanjanchi MA (2003) Anal Chim Acta 491:193
17. Dilgin Y, Dursun Z, Nisli G, Gorton L (2005) Anal Chim Acta 542:162
18. Yang XS, Chen X, Zhang X, Yang WS, Evans DG (2008) Sens Actuators B 129:784
19. Unal U, Matsumoto Y, Tamoto N, Koinuma M, Machida M, Izawa K (2006) J Solid State Chem 179:33
20. Zhang XB, Feng DS, Chen MF, Ding ZD, Tong ZW (2009) J Mater Sci 44:3020. doi:10.1007/s10853-009-3398-7
21. Fang M, Kim CH, Saupe GB, Kim HN, Waraksa CC, Miwa T, Fujishima A, Mallouk TE (1999) Chem Mater 11:1526
22. Yan Y, Zhang M, Gong K, Su L, Guo Z, Mao L (2005) Chem Mater 17:3457
23. Jehng JM, Wachs IE (1991) Chem Mater 3:100
24. Klika Z, Čapková P, Horáková P, Valášková M, Malý P, Macháň R, Pospíšil M (2007) J Colloid Interface Sci 311:14
25. Nakato T, Kusunoki K, Yoshizawa K, Kuroda K, Kaneko M (1995) J Phys Chem 99:17896
26. Ma JJ, Zhang XB, Yan C, Tong ZW, Inoue H (2008) J Mater Sci 43:5534. doi:10.1007/s10853-008-2837-1
27. Ghanadzadeh A, Zeini A, Kashef A, Moghadam M (2008) J Mol Liq 138:100
28. Guo RG, Fan GK, Liu TQ (2000) Acta Chim Sinica 58:636
29. Ramasamy V, Anandalakshmi K (2008) Spectrochim Acta A 70:25
30. He XW, Feng XZ, Shen HX (1995) J Anal Sci 11:1
31. Galagan Y, Su WF (2008) J Photochem Photobiol A Chem 195:378
32. Fergus G, Carla CS, Miguel GN (1994) Langmuir 10:3749
33. Žutić V, Svetličić V, Lovrić M, Ružić I, Chevalet J (1984) J Electroanal Chem 177:253
34. de Araujo Nicolai SH, Rodrigues PRP, Agostinho SML, Rubim JC (2002) J Electroanal Chem 527:103
35. Zhang JD, Zheng YQ, Jiang GD, Yang CZ, Oyama M (2008) Electrochem Commun 10:1038
36. Liao F, Zhu QT, He XY, Ai Z, Cai DC (2007) Chem Rev Appl 19
37. Xian YZ, Liu F, Xian Y, Zhou YY, Jin LT (2006) Electrochim Acta 51:6527
38. Chen HY, Ju HX, Xun YG (1994) Anal Chem 66:4538